

The Evolution of Meson Masses in a Strong Magnetic Field

**M.A.Andreichikov^a B.O.Kerbikov^{a,b,c} E.V.Lushevskaya^{a,b} Yu.A.Simonov^a
O.E.Solovjeva^a**

^a*Institute for Theoretical and Experimental Physics, B. Cheremushkinskaya 25, 117218 Moscow, Russia*

^b*Moscow Institute of Physics and Technology, Institutskiy per. 9, 141700 Dolgoprudniy, Russia*

^c*Lebedev Physical Institute RAS, Leninsky prospekt 53, Moscow, Russia*

E-mail: andreichikov@mail.ru, borisk@itep.ru, lushevskaya@itep.ru,
simonov@itep.ru, olga.solovjeva@itep.ru

ABSTRACT: Spectra of $q\bar{q}$ hadrons are investigated in the framework of the Hamiltonian obtained from the relativistic path integral in external homogeneous magnetic field. The spectra of all 12 spin-isospin s-wave states, generated by π and ρ mesons with different spin projections, are studied both analytically and numerically on the lattice as functions of (magnetic field) eB . Results are in agreement and demonstrate three types of behavior, with characteristic splittings predicted by the theory.

Contents

1	Introduction	1
2	The relativistic Hamiltonian of quark systems	3
3	Meson trajectories in MF	6
4	One-gluon exchange in MF	8
5	Spin-dependent corrections	9
6	Spin-isospin splittings in MF	10
7	Pion chiral degrees of freedom in MF	13
8	Lattice calculations	15
9	Results and discussion	19
A	String tension renormalization in CS method	22
B	The wave function of the neutral meson in CS method	23

1 Introduction

The influence of magnetic field (MF) on the strong interacting particles is an actively discussed topic, see, e.g. a recent review [1]. When MF is not ultra-intense ($eB \ll \sigma$, where $\sigma = 0.18 \text{ GeV}^2$ is a confinement string tension)¹, the main characteristics related to the behavior of hadrons in MF are magnetic moments and magnetic susceptibilities, while for the strong MF limit ($eB \geq \sigma$) the hadron energy and width depend on MF directly.

These topics are important in astrophysics of neutron stars [2], in cosmological theories [3], in atomic physics [4–7] in the physics of heavy ion collisions [8], and in the high-intensity lasers [9].

On the theoretical side the main directions of research in this area are the lattice studies [11]–[17], [18]–[29], the chiral Lagrangians with MF [30]–[33], effective hadron

¹We use relativistic system of units $\hbar = c = 1$, then $1 \text{ GeV}^2 = 5.12 \cdot 10^{19} \text{ G}$

Lagrangians [1, 34],[35]-[38], and recently developed path integral Hamiltonians (PIH) [40]-[46], and the chiral Lagrangian with quark degrees of freedom [47].

The PIH method has appeared to be well suited to the inclusion of an arbitrary external MF. Here one obtains simple expressions for magnetic moments of hadrons, mesons [52] and baryons [53], which are in a good agreement with available experimental and lattice data, as well as with existing model calculations. We stress at this point, that in all calculations done within the PIH framework, the final results are expressed in terms of basic QCD parameters - string tension σ , α_s and current quark masses m_q .

A sample of light neutral meson masses in MF (actually, the meson energies for zero longitudinal momentum) has been calculated with PIH framework in [40-42], and the Nambu-Goldstone (NG) modes in MF have been studied in [47]. In all cases the resulting values of $M_i(B)$ are in reasonable agreement with lattice data from [13]-[14]. The three-body neutral systems in strong MF were studied with PIH in [54], but there is no lattice data now to compare with.

In a general case, solving the spectral problem for hadrons in MF is a cumbersome task. To proceed with analytic calculations, one should use some special techniques. One of them is the Pseudomomentum approach. It was introduced in [55] to separate center-of-mass (c.m.) motion from the relative motion in the nonrelativistic Hamiltonian for the neutral system in MF. This approach was extended to the relativistic sector in the PIH framework for two-body systems in [40-42] and for three-body systems in [56]. The Pseudomomentum approach is applicable only for electrically neutral systems, and for the charged ones an exact analytical answer was obtained only in an unphysical model of charged meson with equally charged quark constituents [41].

Below we are suggesting a new approximate analytic method of constituent separation (CS) that allows to get a quantitative result for any meson masses with 15% accuracy for the strong MF ($eB \gg \sigma$) and with 20% accuracy for $eB < \sigma$. As will be shown, the CS method allows to study charged and neutral systems in the same way. To introduce it, we first write the relativistic Hamiltonian in MF within PIH formalism and exploit the oscillator representation for the confinement interaction used before in [40-42] with 5% accuracy. This allows to split the Hamiltonian into transversal and longitudinal (with respect to the MF direction) parts analytically. All the rest interaction - one-gluon exchange, spin-dependent and self-energy interactions are studied perturbatively.

Our final results for the neutral mesons in MF are obtained in two independent ways: via Pseudomomentum and the CS methods, which allows to check the accuracy of our results.

The paper is organized as follows: in Section 2 we write relativistic Hamiltonian and discuss the main features of CS method. (Details of this method are discussed in Appendix A). As a result we obtain in Section 2 the hadron mass and the ground state wave function as a function of eB and σ for an arbitrary meson in MF. In Section 3

a classification of meson mass trajectories with different spin and isospin projections is given with the corresponding asymptotics in high MF regime $eB \rightarrow \infty$. In Section 4 the perturbative correction due to the one-gluon exchange is calculated and the absence of the color Coulomb collapse is demonstrated. The CS wave function for neutral mesons is discussed in the Appendix B. In Section 5 the spin-spin interaction in MF and the seemingly possible “hyperfine collapse” is discussed. In Section 6 a general discussion of the we spin-isospin splitting is given. In Section 7 we study the chiral and nonchiral treatment of pion masses in MF. In Section 8 the details of our lattice calculations are given. Results of both analytic and lattice results are discussed in the concluding Section 9.

2 The relativistic Hamiltonian of quark systems

We start from the relativistic Hamiltonian of the N-quark system in an external homogeneous MF, which according to [40]-[45] is

$$H_0 = \sum_{i=1}^N \frac{(p_k^{(i)} - e_i A_k)^2 + (m_i^q)^2 + \omega_i^2 - e_i \boldsymbol{\sigma}_i \mathbf{B}}{2\omega_i}, \quad (2.1)$$

where ω_i are virtual quark energies to be intergrated over in the path integral, and m_i^q are current quark masses. At this step we neglect any internal interactions between quarks, i.e. confinement, gluon-exchange, etc. It is convenient to choose symmetrical gauge for MF $\mathbf{A}_i = \frac{1}{2}(\mathbf{B} \times \mathbf{r}_i)$ which allows to define an angular momentum projection m_i for each quark as a quantum number. The spectrum of (2.1) with $m_i = 0$ is

$$\varepsilon_i(\omega_i) = \frac{(m_i^q)^2 + \omega_i^2 + |e_i|B(2n_{\perp i} + 1) - e_i \boldsymbol{\sigma}_i \mathbf{B} + (p_z^{(i)})^2}{2\omega_i}. \quad (2.2)$$

According to [40]-[45] the physical spectrum is given by the stationary point value of ε , with respect to ω_i

$$\left. \frac{d\varepsilon_i(\omega_i)}{d\omega_i} \right|_{\omega_i=\omega_i^{(0)}} = 0, \quad \varepsilon^{(i)}(\omega_i^{(0)}) \equiv \bar{\varepsilon}^{(i)}, \quad \bar{E}_0 \equiv \sum_{i=1} \bar{\varepsilon}_i, \quad (2.3)$$

$$\bar{\varepsilon}_i = \sqrt{(m_i^q)^2 + (p_z^{(i)})^2 + |e_i|B(2n_{\perp} + 1) - e_i \boldsymbol{\sigma}_i \mathbf{B}}.$$

It is easy to see that this spectrum coincides with the solution of the Dirac equation for N non-interacting relativistic particles in MF.

As in [41] we now introduce the confining interaction V_{conf} , which is treated nonperturbatively, while the other interactions like one-gluon exchange V_{OGE} , spin-dependent

interaction a_{SS} and self-energy corrections ΔM_{SE} are treated perturbatively in the next sections. The Hamiltonian becomes

$$H_d = H_0 + V_{\text{conf}} \quad (2.4)$$

with the ground state eigenvalue M_d (nonperturbative, or dynamical mass) and the ground state wave function $|\Psi_0\rangle$. The total meson mass is a sum of M_d and the perturbative corrections

$$M_{\text{total}} = M_d + \langle \Psi_0 | V_{OGE} | \Psi_0 \rangle + \langle a_{SS} \rangle + \Delta M_{SE}. \quad (2.5)$$

One can note, that the contribution of the V_{conf} in strong MF ($eB \gg \sigma$) is negligible in the plane transverse to the MF direction and should be retained only for lowest levels, which we call “zero hadron states” (ZHS) (see below). Another feature is that in strong MF regime the translational invariance of the center-of-mass (c.m.) is broken due to magnetic forces (each quark is placed on its own Landau level), but the confinement still defines the motion of quarks in the direction along the MF.

To simplify calculations we chose the confining term in the variable quadratic form [41, 42], restoring its original linear form at the stationary point (it was checked to be accurate within about 5%), namely

$$V_{\text{conf}}^{(q\bar{q})} = \sigma |\mathbf{r}_1 - \mathbf{r}_2| \rightarrow \frac{\sigma}{2\gamma} (\mathbf{r}_1 - \mathbf{r}_2)^2 + \frac{\sigma\gamma}{2}, \quad (2.6)$$

where γ is variational parameter and $\sigma = 0.18 \text{ GeV}^2$ is a confinement string tension. The dependence of the string tension σ on the MF is caused by the fluctuating $q\bar{q}$ pairs embedded to the string and provides a correction about $\frac{\Delta\sigma}{\sigma} \sim 15\%$ at $eB \sim 1 \text{ GeV}^2$. This phenomenon was studied on the lattice in [43] and was confirmed within PIH formalism in [44]. The correction to the ground state caused by this effect is beyond the declared accuracy and is neglected in what follows. To produce an approximation for the energy, one should minimize the resulting state energy obtained from the Hamiltonian (2.4) with respect to ω_i and γ simultaneously.

The oscillator approximation (2.6) gives an advantage to separate motion along the z axis (parallel to the MF) and in $x - y$ plane

$$\Psi_0 = \psi^{(z)}(z^{(1)}, z^{(2)}) \psi^{(\perp)}(\mathbf{r}_{\perp}^{(1)}, \mathbf{r}_{\perp}^{(2)}); \quad H_d = H_{\perp} + H_3, \quad (2.7)$$

where the motion along the z -axis is defined by the Hamiltonian

$$H_3 = \left(\frac{(p_3^{(1)})^2}{2\omega_1} + \frac{(p_3^{(2)})^2}{2\omega_2} + \frac{\sigma}{2\gamma} (z^{(1)} - z^{(2)})^2 \right) \rightarrow \frac{P_3^2}{2(\omega_1 + \omega_2)} + \frac{\pi_3^2}{2\tilde{\omega}} + \frac{\sigma}{2\gamma} \eta_3^2, \quad (2.8)$$

where we use c.m. reference frame with $P_3 = p_3^{(1)} + p_3^{(2)}$, $\eta_3 = z^{(1)} - z^{(2)}$; $\pi_3 = \frac{1}{i} \frac{\partial}{\partial \eta_3}$, $\tilde{\omega} = \frac{\omega_1 \omega_2}{\omega_1 + \omega_2}$. The longitudinal part of the ground state energy is

$$M_3^0 = \frac{P_3^2}{2(\omega_1 + \omega_2)} + \left(n_3 + \frac{1}{2} \right) \sqrt{\frac{\sigma}{\tilde{\omega}\gamma}}; \quad n_3 = 0; \quad P_3 = 0. \quad (2.9)$$

For the motion in the transversal plane one can use an approximation of decoupled quarks at large MF, making the following substitution

$$(\mathbf{r}_\perp^{(1)} - \mathbf{r}_\perp^{(2)})^2 = (\mathbf{r}_\perp^{(1)} - \mathbf{r}_\perp^0)^2 + (\mathbf{r}_\perp^{(2)} - \mathbf{r}_\perp^0)^2 - 2(\mathbf{r}_\perp^{(1)} - \mathbf{r}_\perp^0)(\mathbf{r}_\perp^{(2)} - \mathbf{r}_\perp^0) \rightarrow \sum_{i=1}^2 (\mathbf{r}_\perp^{(i)} - \mathbf{r}_\perp^0)^2, \quad (2.10)$$

where c.m. position \mathbf{r}_\perp^0 is fixed at the origin in $x - y$ plane. This approximation corresponds to the configuration where the confining string connects each quark to the c.m., i.e. the string is effectively elongated. The magnetic energy of each quark in strong MF (Landau level) is larger than the confining interaction with the factor $\frac{eB}{\sigma}$, which make this approximation legitimate at $eB > \sigma$ regime. To extend our method to the $eB < \sigma$ region, where the behaviour is mostly defined by confinement, one should introduce an effective string tension σ_1 and σ_2 for each part of the string, connecting quarks to the c.m.

$$V_{\text{conf}} = \frac{\sigma_1}{2\gamma} (\mathbf{r}_\perp^{(1)} - \mathbf{r}_\perp^0)^2 + \frac{\sigma_2}{2\gamma} (\mathbf{r}_\perp^{(2)} - \mathbf{r}_\perp^0)^2 + \frac{\sigma\gamma}{2}, \quad (2.11)$$

to compensate an effective string elongation. As shown in Appendix A, the appropriate values of σ_1, σ_2 are

$$\sigma_1 = \frac{\sigma}{1 + \frac{\omega_1}{\omega_2}}; \quad \sigma_2 = \frac{\sigma}{1 + \frac{\omega_2}{\omega_1}}. \quad (2.12)$$

Using this " σ -renormalization" procedure, one can show that the dynamical mass of the ground state M_d , calculated in [41] with the Pseudomomentum technique for neutral mesons, exactly coincides with the dynamical mass obtained in the above CS formalism for the arbitrary value of MF. As a result this approximation make quarks effectively decoupled in $x - y$ plane and one can write

$$\psi^{(\perp)}(\mathbf{r}_\perp^{(1)}, \mathbf{r}_\perp^{(2)}) = \psi_1^{(\perp)}(\mathbf{r}_\perp^{(1)}) \psi_2^{(\perp)}(\mathbf{r}_\perp^{(2)}). \quad (2.13)$$

The transversal part of the hamiltonian H_\perp has the ground state energy

$$M_\perp^0 = \sum_{i=1}^2 \frac{m_i^2 + \omega_i^2 - e_i \sigma_i \mathbf{B} + (2n_\perp^{(i)} + 1) \sqrt{(e_i B)^2 + 4\sigma_i \omega_i / \gamma}}{2\omega_i}; \quad n_\perp^{(i)} = 0, \quad (2.14)$$

where σ_i are given by (2.12). The total dynamical mass is given by the sum

$$M_d = M_\perp^0 + M_3^0 + \frac{\sigma\gamma}{2}. \quad (2.15)$$

The actual trajectories for the dynamical mass in MF, $M_d(eB)$ are obtained using the stationary point conditions in a similar way as (2.3)

$$\tilde{M}_d = M_d^0(\omega_i^{(0)}, \gamma^{(0)}), \quad \left. \frac{\partial M_d}{\partial \gamma} \right|_{\gamma=\gamma^{(0)}} = \left. \frac{\partial M_d}{\partial \omega_i} \right|_{\omega_i=\omega_i^{(0)}} = 0. \quad (2.16)$$

The corresponding wave function for the ground state \tilde{M}_d is

$$\Psi_0 = \left(\frac{\tilde{\omega}^{(0)} \Omega_z}{\pi} \right)^{\frac{1}{4}} \left(\frac{\omega_1^{(0)} \Omega_1 \omega_2^{(0)} \Omega_2}{\pi^2} \right)^{\frac{1}{2}} e^{-\frac{\omega_1^{(0)} \Omega_1}{2} (\mathbf{r}_1^\perp)^2 - \frac{\omega_2^{(0)} \Omega_2}{2} (\mathbf{r}_2^\perp)^2 - \frac{\tilde{\omega}^{(0)} \Omega_z}{2} (\eta_z^2)}, \quad (2.17)$$

where Ω_1 , Ω_2 and Ω_z are harmonic oscillator frequencies

$$\Omega_i = \frac{1}{2\omega_i^{(0)}} \sqrt{(e_i B)^2 + \frac{4\sigma_i \omega_i^{(0)}}{\gamma^{(0)}}}; \quad \Omega_z = \sqrt{\frac{\sigma}{\tilde{\omega}^{(0)} \gamma^{(0)}}}. \quad (2.18)$$

Comparing (2.17) with the same wave function obtained in [41] for neutral mesons one can see that now we have two elongated ellipsoids for each quark instead of one ellipsoid in $\boldsymbol{\eta} = \mathbf{r}_1 - \mathbf{r}_2$, but the resulting spectra coincide.

3 Meson trajectories in MF

We turn now to the general structure of the meson spectrum and the limits of weak ($eB < \sigma$) and strong ($eB \gg \sigma$) MF.

For small MF both γ and ω are independent of MF in the leading order and the lowest order the correction to the dynamical mass is

$$\tilde{M}_d(B) = \tilde{M}_d(B=0) - \sum_{i=1}^2 \frac{e_i \boldsymbol{\sigma}_i \mathbf{B}}{2\omega_i^{(0)}} = \tilde{M}_d(B=0) - \boldsymbol{\mu} \mathbf{B} + c|e\mathbf{B}|, \quad (3.1)$$

where $\boldsymbol{\mu}$ is the magnetic moment of the hadron, and the $c|e\mathbf{B}|$ term is c.m. energy contribution (the lowest Landau level) in MF for the charged mesons (note, that in this paper we discuss only s-wave hadrons and all orbital momenta are zero).

Magnetic moments in PIH formalism have been calculated in [52] for mesons and are in good agreement with experiment and available lattice data. It is easy to see there that for massless quarks the expansion in (3.1) is actually done in powers of $(\frac{eB}{\sigma})$.

For the strong MF limit the situation is more complicated. Confining ourselves to the lowest Landau levels (LLL) for all quarks and antiquarks, i.e. $n_\perp^{(i)} = 0$ in (2.9) and (2.14), we can separate out the hadrons, which consist of only LLL states of both quarks with $e_i \sigma_z^i = |e_i|$, $i = 1, 2$. These states are MF-independent at $eB \rightarrow \infty$ and we shall call them “zero hadron states” (ZHS). Note, that ZHS do not possess definite total spin and isospin quantum numbers.

All other hadron states, except for ZHS, will have energies growing with MF as $\sim \sqrt{|eB|}$ and therefore thermodynamically suppressed at large MF. In the limit of strong MF the dynamical masses for ZHS can be written as

$$M_d^{(ZHS)}(eB \gg \sigma) \simeq M_3^0 + \sum_{i=1}^2 \frac{m_i^2 + \omega_i^2}{2\omega_i} + \frac{\sigma\gamma}{2}. \quad (3.2)$$

The stationary point analysis according to (2.16) for $m_1 = m_2 = 0$, $e_i \sigma_z^i = 1$, $i = 1, 2$, yields

$$\begin{aligned} \omega^{(0)} = \omega_1^{(0)} = \omega_2^{(0)} &= \frac{\sqrt{\sigma}}{2}; \quad \gamma^{(0)} = \frac{1}{\sqrt{\sigma}}; \\ \tilde{M}_d^{ZHS} &= 2\sqrt{\sigma} = 4\omega^{(0)}. \end{aligned} \quad (3.3)$$

The same result was obtained in [40–42, 54] with the Pseudomomentum technique.

We turn now to the meson states still with zero orbital momentum and not belonging to the ZHS states, i.e. violating the equality $\frac{e_i}{|e_i|} \sigma_z^i = 1$. The resulting meson energy according to (2.15)-(2.16) for $m_1 = m_2 = 0$, $P_3 = 0$, $e_1 = |e_1|, e_2 = |e_2|$ is

$$M_d = M_\perp^0 + M_3^0 + \frac{\sigma\gamma}{2} = \frac{\omega_1}{\gamma} + \frac{\sigma}{\gamma e_1 B} + \frac{\sigma}{\gamma e_2 B} + \frac{1}{2} \sqrt{\frac{\sigma}{\tilde{\omega}\gamma}} + \frac{\omega_2^2 + 2e_2 B}{2\omega_2} + \frac{\sigma\gamma}{2}, \quad (3.4)$$

which yields

$$\begin{aligned} \omega_2^{(0)} &= \sqrt{2e_2 B}, \quad \gamma^{(0)} = \frac{1}{\sqrt{2\sigma}}, \quad \omega_1^{(0)} = 2^{-5/6} \sqrt{\sigma}, \\ \tilde{M}_d^I &= \sqrt{2e_2 B} + \sqrt{2\sigma}. \end{aligned} \quad (3.5)$$

The same result occurs when $\frac{e_1}{|e_1|} \sigma_z^1 = -1$, $\frac{e_2}{|e_2|} \sigma_z^2 = 1$ with replacement $e_2 \rightarrow e_1$. Now we turn to the case when both products $\frac{e_1}{|e_1|} \sigma_z^1$ and $\frac{e_2}{|e_2|} \sigma_z^2$ are negative. In this case one obtains

$$\begin{aligned} \omega_i^{(0)} &= \sqrt{2e_i B}, \quad \gamma^{(0)} = 2^{-2/3} (\sigma \tilde{\omega}^{(0)})^{-1/3}, \\ \tilde{M}_d^{II} &= \sqrt{2e_1 B} + \sqrt{2e_2 B} + \frac{3\sigma^{2/3}}{2^{5/3} (\tilde{\omega}^{(0)})^{1/3}}. \end{aligned} \quad (3.6)$$

Thus we have three different asymptotic modes for s-wave meson dynamical masses M_d in MF, classified with respect to spin projections

$$\begin{aligned} 1) \text{ ZHS : } & e_1 \sigma_z^1 > 0, \quad e_2 \sigma_z^2 > 0 : \\ & \tilde{M}_d^{ZHS}(eB \gg \sigma) = 2\sqrt{\sigma}; \\ 2) \text{ I : } & e_1 \sigma_z^1 > 0, \quad e_2 \sigma_z^2 < 0 : \\ & \tilde{M}_d^I(eB \gg \sigma) = \sqrt{2e_1 B} + \sqrt{2\sigma}; \\ 3) \text{ II : } & e_1 \sigma_z^1 < 0, \quad e_2 \sigma_z^2 < 0 : \\ & \tilde{M}_d^{II}(eB \gg \sigma) = \sqrt{2e_1 B} + \sqrt{2e_2 B}. \end{aligned} \quad (3.7)$$

We shall return to this classification later in Section 6 in our study of spin-isospin splittings in weak MF regime.

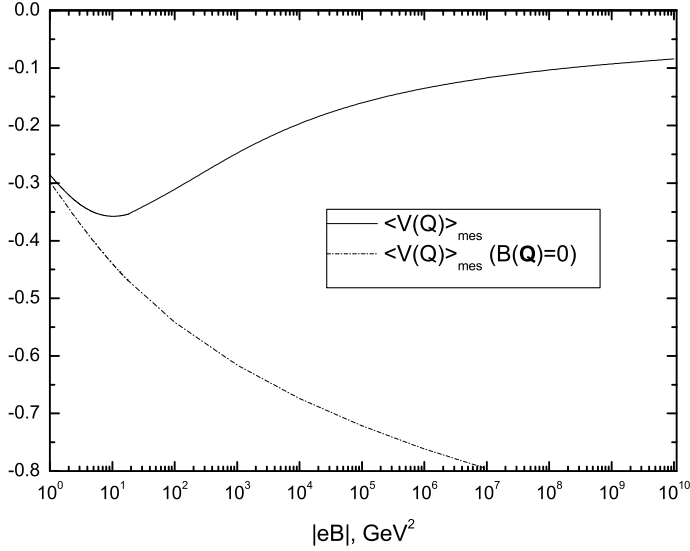


Figure 1. Color Coulomb matrix element $\langle V_{OGE} \rangle$ (in GeV) in MF with screening (solid line) and without screening (dashed line) by $q\bar{q}$ pairs. $\langle V_{OGE} \rangle$ saturates at $eB \rightarrow \infty$ and the fall-to-the-center phenomenon doesn't occur.

4 One-gluon exchange in MF

The first order perturbation correction for one-gluon exchange potential(OGE, or color Coulomb interaction) in MF entering in (2.5) according to [42] is

$$V_{OGE} = - \frac{16\pi\alpha_s^{(0)}}{3 \left[Q^2 \left(1 + \frac{\alpha_s^0}{4\pi} \frac{11}{3} N_c \ln \left(\frac{\mathbf{q}^2 + M_B^2}{\Lambda^2} \right) \right) + \frac{\alpha_s^{(0)} n_f |eB|}{\pi} e^{-\frac{q_1^2}{2|eB|}} T \left(\frac{q_3^2}{4\sigma} \right) \right]}, \quad (4.1)$$

where $N_c = 3$, $n_f = 2$, $\alpha_s^{(0)} = 0.42$, QCD parameter $\Lambda = 0.3 \text{ GeV}$, and the $M_B^2 = 2\pi\sigma = 1.1 \text{ GeV}^2$ preventing Landau singularity was calculated in [51]. Form (4.1) includes screening of the OGE potential by the quark-antiquark pairs created in MF. This effect prevents the “fall-to-the-center” phenomenon for ZHS hadrons in MF, as shown in the Fig.1 and 7. One can see that the matrix element $\langle \Psi | V_{OGE} | \Psi \rangle$ for meson saturates at $eB \sim 10 \text{ GeV}^2$ and the system becomes “asymptotically free” in $eB \rightarrow \infty$ limit when $\langle \Psi | V_{OGE} | \Psi \rangle \rightarrow 0$. The driving force of the Coulomb collapse is an uncontrollable growth of the Coulomb interaction when the system is squeezed by MF

forces. The role of screening of the Coulomb interaction in MF has a long story, see e.g. [4–6] for atomic systems.

The next step is to average the potential (4.1) over the wave function (2.17) obtained by the CS method.

$$\langle V_{OGE} \rangle = \langle \Psi_0 | V_{OGE} | \Psi_0 \rangle = \int d^3\mathbf{r}_1 d^3\mathbf{r}_2 |\Psi_0(\mathbf{r}_1, \mathbf{r}_2)|^2 V_{OGE}(\mathbf{r}_1 - \mathbf{r}_2). \quad (4.2)$$

Separating the integration in $x - y$ plane and in z -direction, one has

$$\langle V_{OGE} \rangle = \int d^2\mathbf{r}_1^\perp d^2\mathbf{r}_2^\perp d\eta_z V_{OGE}(\mathbf{r}_1 - \mathbf{r}_2) |\psi_0^{(1)}(\mathbf{r}_1^\perp)|^2 |\psi_0^{(2)}(\mathbf{r}_2^\perp)|^2 |\psi_0^{(z)}(\eta_z)|^2. \quad (4.3)$$

In the momentum space one obtains

$$\langle V_{OGE} \rangle = \frac{1}{(2\pi)^3} \int d^3\mathbf{q} V(\mathbf{q}) F[|\psi_0^{(1)}|^2]_{-\mathbf{q}_\perp} F[|\psi_0^{(2)}|^2]_{\mathbf{q}_\perp} F[|\psi_0^{(z)}|^2]_{q_z} \quad (4.4)$$

where $F[\dots]$ are Fourier images

$$F[|\psi_0^{(i)}|^2]_{\mathbf{p}_\perp} = \int d^2\mathbf{x}_\perp |\psi_0^{(i)}(\mathbf{x}_\perp)|^2 e^{i\mathbf{P}_\perp \cdot \mathbf{x}_\perp} = e^{-\frac{(\mathbf{P}_\perp^i)^2}{4\omega_i^{(0)}\Omega_i}}; \quad (4.5)$$

$$F[|\psi_0^{(z)}|^2]_{\pi_z} = \int d\eta_z |\psi_0^{(z)}(\eta_z)|^2 e^{ip_z\eta_z} = e^{-\frac{\pi_z^2}{4\bar{\omega}^{(0)}\Omega_z}}, \quad (4.6)$$

where Ω_i and Ω_z are given by (2.18). Comparing this result in case of the neutral meson with the exact one, obtained with Pseudomomentum procedure, one has to make a correction for the wave function, see Appendix B for details.

5 Spin-dependent corrections

A detailed review of the spin-dependent forces in PIH framework is given in [57]. Here we only emphasize that the spin-dependent perturbative corrections arise from the $\langle \sigma_i F \cdot \sigma_j F \rangle$ correlators, where σ_i are Clifford 4×4 $\sigma_{\mu\nu}$ for i -th quark constituent and F are non-abelian field strength tensors.

Averaging over the stochastic gluonic background field, one has two types of corrections – the self-energy term for $i = j$ and color-magnetic spin-spin interaction terms for $i \neq j$, where i, j are quark numbers

$$\begin{aligned} \Delta M_{SE} &= -\frac{4\sigma}{3\pi\omega_i^{(0)}}; \\ V_{SS}^{ij} &= \frac{8\pi\alpha_s^{(0)}}{9\omega_i^{(0)}\omega_j^{(0)}} \delta(\mathbf{r}_i - \mathbf{r}_j) (\boldsymbol{\sigma}_i \cdot \boldsymbol{\sigma}_j). \end{aligned} \quad (5.1)$$

The self-energy correction ΔM_{SE} in (5.1) was used in a large number of calculations [59], confirmed by the experimental data and lattice simulations. In case of an external MF we retain in ΔM_{SE} the value $\omega_i^{(0)} = \omega_i^{(0)}(eB = 0)$, instead of $\omega_i^{(0)}(eB)$, which does not change appreciably M_{total} .

A different story is for the spin-spin interaction in (5.1). As it was shown in [7, 41, 57], the wave function of hadronic and atomic systems becomes “focused” at the origin by MF, i.e. $|\Psi_0(0)|^2 \sim eB$ for large MF value. This “magnetic focusing” phenomenon could induce the fall-to-the-center phenomenon for the lowest lying ZHS states. However, as shown in [57], the colormagnetic fields cannot violate the positivity of the $q\bar{q}$ spectra, implying that some sort of the cut-off parameter must occur in the whole perturbative series with nonperturbative background. Moreover, PIH method has a natural dimensional cutoff parameter for color field $\lambda \simeq 1 \text{ GeV}^{-1}$ – correlation length of the vacuum gluonic background, which should be used to smear δ -function in (5.1) [58]

$$\delta(\mathbf{r}) \rightarrow \frac{1}{\pi^{3/2}\lambda^3} e^{-\frac{\mathbf{r}^2}{\lambda^2}}, \quad (5.2)$$

and after the averaging with the CS meson wave function (2.17) one obtains the spin-spin matrix element

$$\begin{aligned} \langle a_{SS} \rangle (\boldsymbol{\sigma}_1 \cdot \boldsymbol{\sigma}_2) &= \int V_{SS}^{12} |\Psi_0|^2 d^3\mathbf{r}_1 d^3\mathbf{r}_2 = \\ &= \frac{1}{\sqrt{\pi^3\lambda^6}} \frac{\sqrt{\tilde{\omega}^{(0)}\Omega_z}}{\sqrt{\frac{1}{\lambda^2} + \tilde{\omega}^{(0)}\Omega_z}} \frac{1}{1 + \frac{1}{\lambda^2} \frac{\omega_1^{(0)}\Omega_1 + \omega_2^{(0)}\Omega_2}{\omega_1^{(0)}\Omega_1 \omega_2^{(0)}\Omega_2}} \frac{8\pi\alpha_s^{(0)}}{9\omega_1^{(0)}\omega_2^{(0)}} (\boldsymbol{\sigma}_1 \cdot \boldsymbol{\sigma}_2). \end{aligned} \quad (5.3)$$

Smearing procedure prevents the collapse of the meson in strong MF and it stops the unbounded fall of the total mass value in increasing MF.

It is important to notice here that the approximation of the confinement potential by the harmonic oscillator potential (2.6) gives too small value for $|\Psi_0(0)|^2$ and the hyperfine splitting $\Delta E = 4\langle a_{SS} \rangle$ between the non-chiral π^- and ρ^- mesons at $eB = 0$ is too small (see Fig. 3 and 7) as compared with realistic case of linear interaction. Moreover, the pion mass at $eB = 0$ is additionally shifted down by chiral dynamics, which we shall take into account in Section 7.

6 Spin-isospin splittings in MF

As pointed out in Section 1, MF violates spin and isospin symmetries, therefore π^0 , ρ^0 split into 8 states and each π^+ , ρ^+ and π^- , ρ^- states split into 4 states in MF correspondingly. Using the asymptotics (3.7), obtained in Section 3 for strong MF regime,

one has

$$\begin{aligned}
1) \rho^+(s_z = 1) &= |u \uparrow \bar{d} \uparrow\rangle \text{ ZHS} \\
2) \rho^+(s_z = -1) &= |u \downarrow \bar{d} \downarrow\rangle \text{ II} \\
3) \rho^+(s_z = 0) &= \frac{1}{\sqrt{2}} (|u \uparrow \bar{d} \downarrow\rangle + |u \downarrow \bar{d} \uparrow\rangle) \text{ I} \\
4) \pi^+(s_z = 0) &= \frac{1}{\sqrt{2}} (|u \uparrow \bar{d} \downarrow\rangle - |u \downarrow \bar{d} \uparrow\rangle) \text{ I} \\
5) \rho^0(s_z = 1) &= \frac{1}{\sqrt{2}} (|u \uparrow \bar{u} \uparrow\rangle + |d \uparrow \bar{d} \uparrow\rangle) \text{ I} \\
6) \rho^0(s_z = -1) &= \frac{1}{\sqrt{2}} (|u \downarrow \bar{u} \downarrow\rangle + |d \downarrow \bar{d} \downarrow\rangle) \text{ I} \\
7) \rho^0(s_z = 0) &= \frac{1}{\sqrt{2}} \left[\frac{1}{\sqrt{2}} (|u \uparrow \bar{u} \downarrow\rangle + |d \uparrow \bar{d} \downarrow\rangle) + \frac{1}{\sqrt{2}} (|u \downarrow \bar{u} \uparrow\rangle + |d \downarrow \bar{d} \uparrow\rangle) \right] \text{ ZHS + II} \\
8) \pi^0(s_z = 0) &= \frac{1}{\sqrt{2}} \left[\frac{1}{\sqrt{2}} (|u \uparrow \bar{u} \downarrow\rangle + |d \uparrow \bar{d} \downarrow\rangle) - \frac{1}{\sqrt{2}} (|u \downarrow \bar{u} \uparrow\rangle + |d \downarrow \bar{d} \uparrow\rangle) \right] \text{ ZHS + II} \\
9) \rho^-(s_z = 1) &= |d \uparrow \bar{u} \uparrow\rangle \text{ II} \\
10) \rho^-(s_z = -1) &= |d \downarrow \bar{u} \downarrow\rangle \text{ ZHS} \\
11) \rho^-(s_z = 0) &= \frac{1}{\sqrt{2}} (|d \uparrow \bar{u} \downarrow\rangle + |d \downarrow \bar{u} \uparrow\rangle) \text{ I} \\
12) \pi^-(s_z = 0) &= \frac{1}{\sqrt{2}} (|d \uparrow \bar{u} \downarrow\rangle - |d \downarrow \bar{u} \uparrow\rangle) \text{ I}
\end{aligned} \tag{6.1}$$

Here on the l.h.s we have the standard spin-isospin configurations for mesons at zero MF, and on the r.h.s we have asymptotic classification according to (3.7) in strong MF for the corresponding states. The states 1)-4), 5)-8) and 9)-12) are composed of quarks and antiquarks in the combinations which yield the required spin and isospin values of π and ρ mesons at $eB = 0$.

With increasing MF the eigenvalues of the total Hamiltonian (2.5) at nonzero MF demonstrate two types of phenomena: a) the mixing effect, due to spin-spin forces, equivalent to the Stern–Gerlach phenomenon, when the MF eigenstate can be expanded in two $eB = 0$ eigenstates; b) the splitting effect, when the zero MF state composed of $u\bar{u}$ and $d\bar{d}$ components, splits into two trajectories due to isospin flavor. Finally, the trajectories for charged mesons like $\rho^+(s_z = 1)$ and $\rho^+(s_z = -1)$ starting at the same mass at $eB = 0$, split into two for $eB > 0$.

To take into account the spin-spin interaction, we choose the basis states $|++\rangle$, $|+-\rangle$, $|-+\rangle$, $|--\rangle$ in spin space. The states 1) and 2), that corresponds to $\rho^+(s_z = 1)$ and $\rho^+(s_z = -1)$ mesons at $eB = 0$ correspondingly, are diagonal and their dynamical

masses are

$$\begin{aligned} M_d^{++} &= \langle ++ | H_d | ++ \rangle; \\ M_d^{--} &= \langle -- | H_d | -- \rangle. \end{aligned} \quad (6.2)$$

After the stationary point analysis (2.16) one has two sets of parameters $(\omega_1^{++(0)}, \omega_2^{++(0)})$ and $(\omega_1^{--(0)}, \omega_2^{--(0)})$. The total mass of these states according to PIH formalism are given by

$$\begin{aligned} M_{total}(\rho^+(s_z = 1)) &= (M_d^{++} + \langle V_{OGE} \rangle + \Delta M_{SE} - \langle a_{SS} \rangle)|_{\omega_1^{++(0)}, \omega_2^{++(0)}}; \\ M_{total}(\rho^+(s_z = -1)) &= (M_d^{--} + \langle V_{OGE} \rangle + \Delta M_{SE} - \langle a_{SS} \rangle)|_{\omega_1^{--(0)}, \omega_2^{--(0)}}, \end{aligned} \quad (6.3)$$

$M_{total}(\rho^+(s_z \pm 1))$ gives rise to two trajectories in MF starting at ρ^+ meson mass at $eB = 0$.

The behavior of states 3) and 4) corresponding to $\rho^+(s_z = 0)$ and π^+ at zero MF is more complicated. These states are composed of $|u \downarrow \bar{d} \uparrow\rangle = | - + \rangle$ and $|u \uparrow \bar{d} \downarrow\rangle = | + - \rangle$ combinations at $eB = 0$. When the MF increases, the states start to mix in the mutually orthogonal combinations

$$\pi^+, \rho^+(s_z = 0) = \alpha \left(\frac{|u \uparrow \bar{d} \downarrow\rangle + |u \downarrow \bar{d} \uparrow\rangle}{\sqrt{2}} \right) + \beta \left(\frac{|u \uparrow \bar{d} \downarrow\rangle - |u \downarrow \bar{d} \uparrow\rangle}{\sqrt{2}} \right). \quad (6.4)$$

The basis vectors are equal to the π^+ and $\rho^+(s_z = 0)$ states at $eB = 0$. The mixing phenomenon is defined by the non-diagonal spin-spin matrix elements

$$\begin{aligned} a_{12} &= \langle + - | \langle a_{SS} \rangle (\boldsymbol{\sigma}_1 \cdot \boldsymbol{\sigma}_2) | - + \rangle |_{\omega_1^{+- (0)}, \omega_2^{+- (0)}}; \\ a_{21} &= \langle - + | \langle a_{SS} \rangle (\boldsymbol{\sigma}_1 \cdot \boldsymbol{\sigma}_2) | + - \rangle |_{\omega_1^{-+ (0)}, \omega_2^{-+ (0)}}; \end{aligned} \quad (6.5)$$

The dynamical masses and the parameters $(\omega_1^{+- (0)}, \omega_2^{+- (0)})$, $(\omega_1^{-+ (0)}, \omega_2^{-+ (0)})$ are defined by the stationary point analysis for the M_d^{+-} , M_d^{-+} and the diagonal elements

$$\begin{aligned} M_{total}^{11} &= (M_d^{+-} + \langle V_{OGE} \rangle + \Delta M_{SE} - \langle a_{SS} \rangle)|_{\omega_1^{+- (0)}, \omega_2^{+- (0)}}; \\ M_{total}^{22} &= (M_d^{-+} + \langle V_{OGE} \rangle + \Delta M_{SE} - \langle a_{SS} \rangle)|_{\omega_1^{-+ (0)}, \omega_2^{-+ (0)}}. \end{aligned} \quad (6.6)$$

The final step is to diagonalize the total mass matrix

$$\begin{bmatrix} M_{total}^{11} & 2a_{12} \\ 2a_{21} & M_{total}^{22} \end{bmatrix} \quad (6.7)$$

and to calculate mixing coefficients

$$\alpha, \beta(\rho^+(s_z = 0)) = \frac{1}{\sqrt{2}} \frac{1 \pm \frac{M_{total}^{11} - E_1}{a_{12}}}{\sqrt{1 + \left(\frac{M_{total}^{11} - E_1}{a_{12}}\right)^2}}; \quad (6.8)$$

$$\alpha, \beta(\pi^+) = \frac{1}{\sqrt{2}} \frac{1 \pm \frac{M_{total}^{11} - E_2}{a_{12}}}{\sqrt{1 + \left(\frac{M_{total}^{11} - E_2}{a_{12}}\right)^2}}$$

The eigenvalues for (6.7) are

$$E_{1,2} = \frac{1}{2}(M_{total}^{11} + M_{total}^{22}) \pm \sqrt{\left(\frac{M_{total}^{22} - M_{total}^{11}}{2}\right)^2 + 4a_{12}a_{21}}. \quad (6.9)$$

The trajectory E_1 with "+" sign in (6.9) starts from the $\rho^+(s_z = 0)$ mass at $eB = 0$ and grows with MF, and the trajectory E_2 with "-" sign corresponds to the π^+ at zero MF. The states E_1 and E_2 are mixtures of π^+ and $\rho^+(s_z = 0)$ at $eB \neq 0$ with mixing coefficients defined by (6.8).

One can define the states 1)-4) with the same isospin structure as quartet (π^+, ρ^+) . States 9)-12) also form the quartet (π^-, ρ^-) with the dynamics in MF the same as for (π^+, ρ^+) if one changes spins and charge signs to the opposite. The states 5)-8) are composed of $u\bar{u}$ and $d\bar{d}$ configurations in isospin. Since the relativistic Hamiltonian is diagonal in isospin, one can split these states into two independent quartets $(\pi^0, \rho^0)(u\bar{u})$ and $(\pi^0, \rho^0)(d\bar{d})$. The diagonal state 5) splits into two trajectories $\rho^0(s_z = 1) = |u \uparrow \bar{u} \uparrow\rangle$ from quartet $(\pi^0, \rho^0)(u\bar{u})$ and $\rho^0(s_z = 1) = |d \uparrow \bar{d} \uparrow\rangle$ from quartet $(\pi^0, \rho^0)(d\bar{d})$ starting from the $\rho^0(s_z = 1)$ mass at zero MF. The same situation holds for the state 6). The states 7)-8) demonstrate the most complicated behaviour in MF: a) the double splitting in isospin to $u\bar{u}$ and $d\bar{d}$ trajectories; b) the mixing in spin $\alpha|u \uparrow \bar{u} \downarrow\rangle + \beta|u \downarrow \bar{u} \uparrow\rangle$ due to spin-spin matrix elements.

7 Pion chiral degrees of freedom in MF

Unlike ρ mesons, the pions obey the chiral dynamics and therefore one should take into account how it changes under the influence of MF. This topic was studied in [47] and here we exploit the results of [47] for neutral and charged pions. The most important feature of these results is that the GMOR relations [61] are kept valid for neutral pions in arbitrary strong MF, while they are violated for charged pions. At the same time at zero and small MF ($eB < f_\pi^2$) the pion mass is defined by GMOR relations both in the neutral and charged case, $m_\pi^2 = \frac{m_q \langle \bar{q}q \rangle}{f_\pi^2}$.

This last dependence $m_\pi^2 \sim O(m_q)$ defines the main difference between chiral and nonchiral pion trajectories.

We start with the neutral pion case, with the standard GMOR relations.

$$m_\pi^2 f_\pi^2 = \bar{m} |\langle u\bar{u} + d\bar{d} \rangle|; \quad \bar{m} = \frac{m_u + m_d}{2}, \quad (7.1)$$

where f_π^2 is given in [18, 62],

$$f_\pi^2 = N_c M^2(0) \sum_{n=0}^{\infty} \left(\frac{\frac{1}{2} |\psi_{n,i}^{(+)}(0)|^2}{(m_{n,i}^{(+)})^3} + \frac{\frac{1}{2} |\psi_{n,i}^{(-)}(0)|^2}{(m_{n,i}^{(-)})^3} \right), \quad (7.2)$$

where $M(0)$ is the confining kernel, $M(0) = \sigma\lambda \cong 0.15$ GeV, and $\langle u\bar{u} \rangle$, $\langle d\bar{d} \rangle$ are quark condensates in MF

$$\langle q\bar{q} \rangle_i = N_c M(0) \sum_{n=0}^{\infty} \left(\frac{\frac{1}{2} |\psi_{n,i}^{(+)}(0)|^2}{m_{n,i}^{(+)}} + \frac{\frac{1}{2} |\psi_{n,i}^{(-)}(0)|^2}{m_{n,i}^{(-)}} \right). \quad (7.3)$$

Here $(+)$ and $(-)$ are individual quark's spin projections and e.g. $\psi_{n,i}^{(-)}$ is the full set of $q\bar{q}$ non-chiral wave functions obtained with PIH formalism, n is the radial quantum number, see [18, 62] for details.

Since $m_{n,i}^{(-)}$ is fast growing with eB , one can retain in the sums (7.2),(7.3) only the $(+)$ terms, and obtain as in [47] the asymptotic behavior of the π^0 mass as $m_{\pi^0}^2 = \frac{\bar{m}}{M(0)} (\bar{m}^{(+)})^2$, where $\bar{m}^{(+)}$ is close to the lowest mass $m_{n,i}$.

It can be seen that all formulae in derivation of the ECL in [47] are diagonal in isospin flavor, so one can write an independent GMOR relation for each $\pi^0(u\bar{u})$ and $\pi^0(d\bar{d})$ mesons, that should split in MF according to (6.1)

$$\begin{aligned} m_{\pi(q\bar{q})}^2 f_{\pi(q\bar{q})}^2 &= m_q |\langle q\bar{q} \rangle|; \\ m_{\pi(q\bar{q})}^2 &= \frac{m_q}{M(0)} \left(m_{(q\bar{q})}^{(+)} \right)^2 |\langle q\bar{q} \rangle|, \quad q = u, d \end{aligned} \quad (7.4)$$

The result of the calculation for $\pi^0(u\bar{u})$ (solid line) according to (7.4) is shown in the Fig.2.

In the case of the charged pions, π^+ and π^- , the situation is drastically different, since they loose their chiral properties at large $eB > \sigma$, and their asymptotics is defined by the independent u and \bar{d} quarks (for π^+), the mode I in (3.7), splitted in two trajectories, $M_{+-}(eB \gg \sigma) \approx \sqrt{\frac{2}{3}}eB$ for π^+ and $M_{-+}(eB \gg \sigma) \approx \sqrt{\frac{4}{3}}eB$ for ρ^+ due to the $\pi^+ - \rho^+$ mixing effect mentioned in Section 6. Taking into account the GMOR relations for $eB = 0$ ($eB < f_\pi^2$), the asymptotics for the charged pions can be written as

$$M_{+-}(B) = \sqrt{m_\pi^2(0) + \frac{2}{3}eB}, \quad (7.5)$$

where $m_\pi^2(0)$ is the pion mass at $eB = 0$.

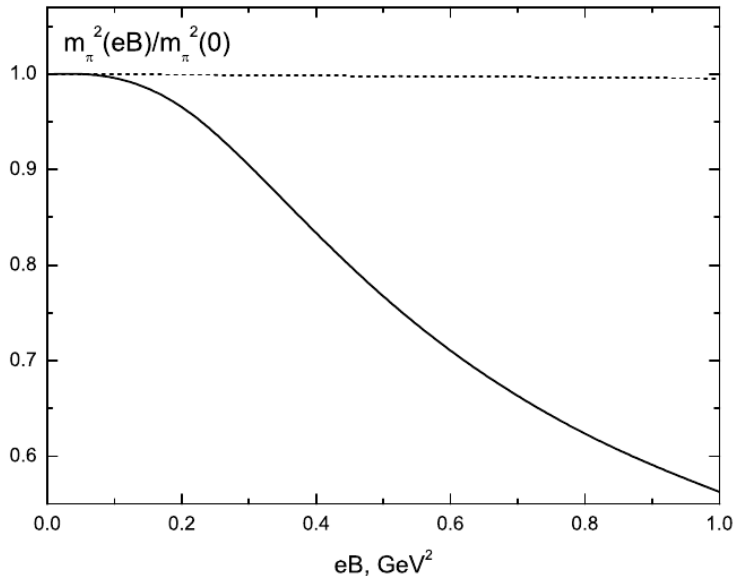


Figure 2. Mass evolution of the chiral π^0 meson in MF from analytic PIH formalism.

In Fig.3 we plot the trajectory of $M_{+-}(B)$ and our lattice data together with the lattice data from [28].

One can summarize our method of chiral meson mass calculation as follows. First, one calculates the spectrum of non-chiral ("spectator") meson masses $m_{n,i}^{(+-)}$ in the MF. Second, one uses (7.2), (7.3) to obtain f_π^2 and $\langle q\bar{q} \rangle$ as functions of eB . Finally, one exploits GMOR relations to extract the resulting chiral mass dependence on eB . The formalism of (7.2), (7.3) was checked without MF in [63, 64], the resulting MF dependence of f_π^2 and $\langle q\bar{q} \rangle$ was checked vs. lattice data in [47, 65].

Summarizing the results for neutral and charged pions one can say that our theoretical predictions are supported by lattice data, and indeed charged and neutral pions behave quite differently at large MF, violating and not violating respectively the GMOR relations.

8 Lattice calculations

The ground state energies of π and ρ mesons are calculated in SU(3) lattice gauge theory without dynamical quarks. Technical details were presented in our previous work [19, 20]. We use 198-336 lattice gauge configurations on the lattice with spacing $a = 0.115 fm$ and 195 configurations for $a = 0.095 fm$ in volume 18^4 . Solving the Dirac equation

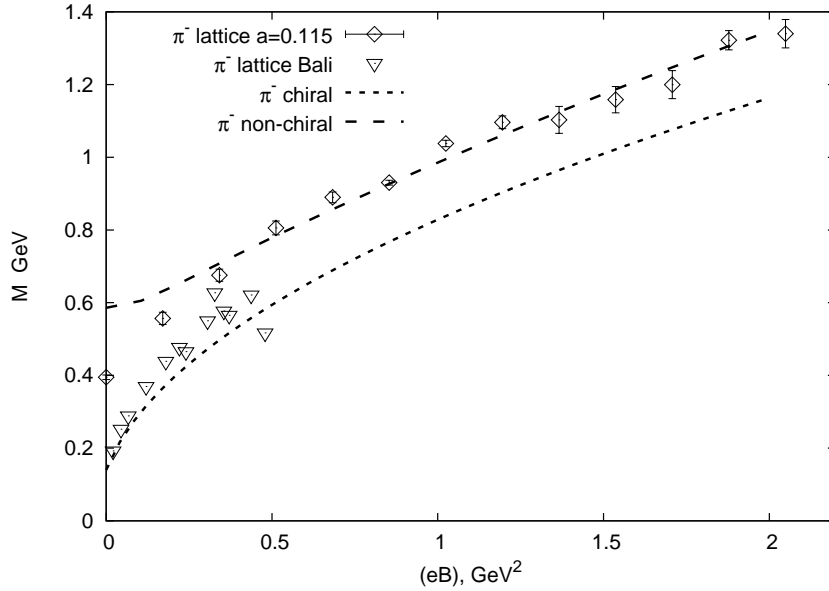


Figure 3. Mass evolution of the chiral (solid line) and nonchiral (dashed line) π^- meson in MF in comparison with the lattice data: triangles [28] and quadrangles with lattice spacing $a = 0.115 fm$ (present paper).

numerically

$$D\psi_k = i\lambda_k\psi_k, \quad D = \gamma^\mu(\partial_\mu - iA_\mu), \quad (8.1)$$

we found eigenfunctions ψ_k and eigenvalues λ_k for a quark in the background gauge field A_μ . Two types of quarks u and d are considered, which are degenerate in mass. An abelian MF interacts with quarks, so $U(1)$ gauge field is introduced into the lattice version of the Dirac operator D [26]

$$\begin{aligned} A_{\mu ij} &= A_{\mu ij}^{SU(3)} + A_\mu^B \delta_{ij}, \\ A_\mu^B(x) &= \frac{B}{2}(x_1\delta_{\mu,2} - x_2\delta_{\mu,1}). \end{aligned} \quad (8.2)$$

Quark fields obey periodic boundary conditions in space and antiperiodic boundary conditions in time. The MF is quantized in a finite lattice volume. Its value is determined by the following formula

$$eB = \frac{6\pi k}{(aL)^2}, \quad k \in Z, \quad (8.3)$$

where e is the elementary charge. Taking the average over the background field A we introduce the correlators in coordinate space

$$\langle \psi^\dagger(x)O_1\psi(x)\psi^\dagger(y)O_2\psi(y) \rangle_A, \quad (8.4)$$

where $O_1, O_2 = \gamma_5, \gamma_\mu$ are Dirac matrices, $\mu, \nu = 1, \dots, 4$ are Lorentz indices, x and y are lattice coordinates.

We performed the numerical Fourier transform of (8.4) in spatial discrete coordinates and set $\langle \mathbf{p} \rangle = 0$ since we are interested in the meson ground state energy. To obtain the masses we expand the correlation function $\tilde{C}(n_t)$ into the exponential series

$$\langle \psi^\dagger(\mathbf{0}, n_t) O_1 \psi(\mathbf{0}, n_t) \psi^\dagger(\mathbf{0}, 0) O_2 \psi(\mathbf{0}, 0) \rangle_A = \sum_k \langle 0 | O_1 | k \rangle \langle k | O_2^\dagger | 0 \rangle e^{-n_t a E_k}. \quad (8.5)$$

When the lattice time n_t is large, the main contribution to the correlator (8.5) comes from the ground state. Due to the periodic boundary conditions the correlator has the following form

$$\tilde{C}_{fit}(n_t) = A_0 e^{-n_t a E_0} + A_0 e^{-(N_T - n_t) a E_0} = 2A_0 e^{-N_T a E_0 / 2} \cosh\left(\left(\frac{N_T}{2} - n_t\right) a E_0\right), \quad (8.6)$$

where A_0 is a constant, E_0 is the ground state energy, a is the lattice spacing. We find the energy E_0 , as a fit parameter, fitting the lattice correlators by formula (8.6). In order to minimize the errors and to exclude the contribution of excited states we take various values of n_t from the interval $5 \leq n_t \leq N_T - 5$. The energy of the charged pion is calculated from the correlation function

$$C^{\pi^\pm} = \langle \bar{\psi}_d(\vec{0}, n_t) \gamma_5 \psi_u(\vec{0}, n_t) \bar{\psi}_u(\vec{0}, 0) \gamma_5 \psi_d(\vec{0}, 0) \rangle. \quad (8.7)$$

Fig.3 shows the energy of a charged pion for the lattice volume 18^4 , the lattice spacing 0.115 fm and the quark masses 17.13 MeV, which corresponds to the pion mass $m_\pi = 395$ MeV at zero MF. The resultant energy increases with the MF value. Errors were obtained through the χ^2 method. According to the exponential fall of the correlator (8.6) at large E , the absolute error of E should grow with energy. However, we do not see this tendency clearly since different number of gauge configurations were utilized for different values of the MF. These numbers are shown in Table 1 in case of the charged meson. We observed an increase of the error for the MF values $eB > 1.2$ GeV², presumably due to the worst convergence of our numerical procedure at high MF values and small quark masses. In Fig.4 we show the correlation functions for different MF values for comparison.

The energy of neutral pion was calculated using the correlation function

$$C^{\pi^0} = (\langle \bar{\psi}_d(\vec{0}, n_t) \gamma_5 \psi_d(\vec{0}, n_t) \bar{\psi}_d(\vec{0}, 0) \gamma_5 \psi_d(\vec{0}, 0) \rangle + \langle \bar{\psi}_u(\vec{0}, n_t) \gamma_5 \psi_u(\vec{0}, n_t) \bar{\psi}_u(\vec{0}, 0) \gamma_5 \psi_u(\vec{0}, 0) \rangle) / \sqrt{2} \quad (8.8)$$

The resultant energies for the $\pi^0(u\bar{u})$ and $\pi^0(d\bar{d})$ configurations diminish with the increase of the MF as shown in Fig.5-6.

$eB, \text{ GeV}^2$	N_{conf}	$E_{\pi^\pm}, \text{ GeV}$	Error
0	245	0.395	0.006
0.171	235	0.557	0.017
0.341	245	0.675	0.017
0.512	311	0.806	0.019
0.683	198	0.890	0.015
0.854	241	0.930	0.007
1.024	232	1.038	0.009
1.195	238	1.096	0.017
1.366	320	1.103	0.037
1.537	333	1.158	0.036
1.707	336	1.200	0.039
1.877	248	1.322	0.027
2.049	244	1.340	0.039
2.220	249	1.476	0.061

Table 1. The values of the π^\pm energy, its errors and the number of lattice configurations, which were used for the calculations at lattice volume 18^4 , lattice spacing $a = 0.115$ fm, bare quark mass 17.13 MeV and various MF values.

The correlation functions of charged ρ mesons for three spatial directions are given by the following relations

$$C_{xx}^{VV} = \langle \bar{\psi}_u(\mathbf{0}, n_t) \gamma_1 \psi_u(\mathbf{0}, n_t) \bar{\psi}_d(\mathbf{0}, 0) \gamma_1 \psi_d(\mathbf{0}, 0) \rangle, \quad (8.9)$$

$$C_{yy}^{VV} = \langle \bar{\psi}_u(\mathbf{0}, n_t) \gamma_2 \psi_u(\mathbf{0}, n_t) \bar{\psi}_d(\mathbf{0}, 0) \gamma_2 \psi_d(\mathbf{0}, 0) \rangle, \quad (8.10)$$

$$C_{zz}^{VV} = \langle \bar{\psi}_u(\mathbf{0}, n_t) \gamma_3 \psi_u(\mathbf{0}, n_t) \bar{\psi}_d(\mathbf{0}, 0) \gamma_3 \psi_d(\mathbf{0}, 0) \rangle. \quad (8.11)$$

If an abelian MF is directed along the 'z' axis, the ρ meson energy with $s_z = 0$ spin projection to the MF direction is determined by the C_{zz}^{VV} correlator. The ground state energies of the ρ meson with spin projections $s_z = +1$ and $s_z = -1$ are determined by the following combinations of correlators

$$C^{VV}(s_z = \pm 1) = C_{xx}^{VV} + C_{yy}^{VV} \pm i(C_{xy}^{VV} - C_{yx}^{VV}). \quad (8.12)$$

We have obtained that the energy of the ρ^- meson with the spin projection $s_z = -1$ diminishes as a function of eB . Fig.7 shows that the energies of ρ^- meson with spin projections $s_z = 0$ and $s_z = +1$ increase with the magnetic field value. The energy of the neutral ρ meson was calculated similarly to the charged ρ meson, but in formulae (8.9), (8.10) and (8.11) one has to consider the sum of the correlators for u and d quarks. In Fig.5-6 we represent the energy of neutral ρ meson with various spin projections. The energies with $s_z = -1$ and $s_z = +1$ increase with the MF and coincide with each other.

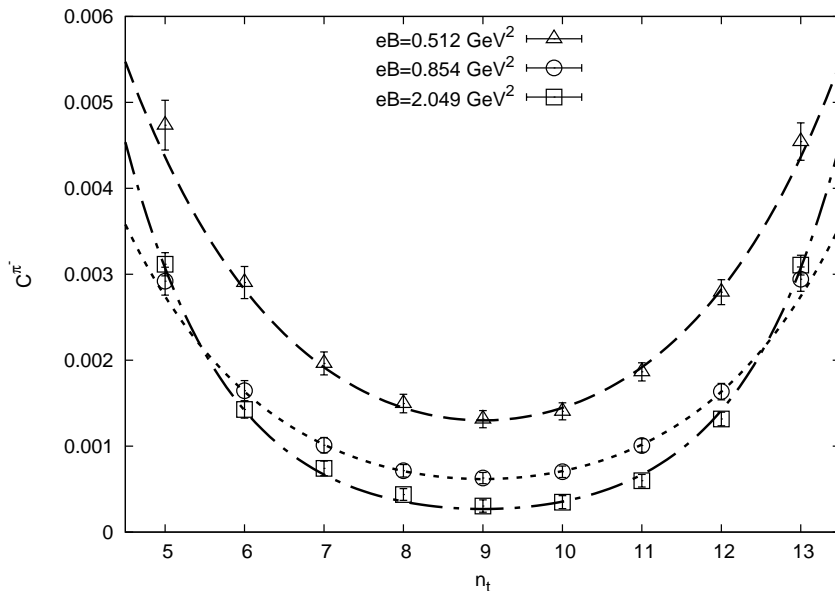


Figure 4. The correlation function (8.7) versus n_t for the lattice spacing 0.115 fm, lattice volume 18^4 and bare quark masses 17.13 MeV for several values of magnetic field eB .

9 Results and discussion

Our paper contain analytic and numerical lattice results for all 12 π, ρ mass trajectories as functions of eB . The main difficulty with analytic results was threefold. First of all, for charged states there is no universal method of the separation of c.m. and relative coordinates (unlike the case of neutral mesons), and therefore we have used a new special (however approximate, $O(15\%)$) approach, called the CS formalism. Secondly, strong MF in lowest approximation brings in vacuum instability due to OGE forces and due to the hyperfine interaction, both growing fast with eB . We have eliminated the OGE instability taking into account the screening effect [42], as was shown in Section 4, see also Fig.1. For the hyperfine problem we have used the stability theorem of [47], ensuring the nonnegativity of hadron masses in the magnetic field, which implies that in higher order the combined nonperturbative and perturbative effects must stabilize hyperfine interaction. To this end we have employed the smearing radius of the hyperfine term of the order of vacuum correlation length $\lambda \simeq 0.2 fm$. Note, that this problem exists also without MF and is usually solved in the same way.

Thirdly, the chiral dynamics, which governs pions at zero MF, may be violated by MF, and this was explicitly demonstrated in [52]. Accordingly we had to consider separately charged and neutral pions, where only the latter keep the the chiral properties, see Fig.2 and 3.

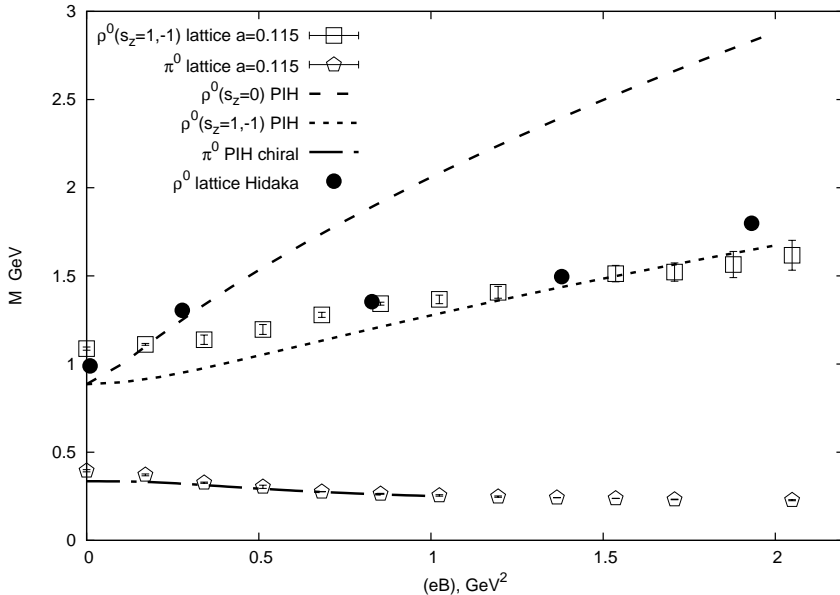


Figure 5. Mass evolution of $(\pi^0, \rho^0)(u\bar{u})$ quartet in MF from analytic (PIH) and lattice data (black circles are from [27]).

Indeed we show in Fig.5 and 6 the behaviour of the $\pi^0(u\bar{u})$ and $\pi^0(d\bar{d})$ masses in MF, which follows from the GMOR relation, where both $f_\pi(eB)$, and $\langle q\bar{q} \rangle(eB)$ are calculated via non-chiral $q\bar{q}$ eigenvalues in MF. Note, that the chiral π^0 mass in Fig.2 and the nonchiral π^0 mass are similar in behavior but differ in scale. The latter is due to fact, that in chiral dynamics m_π^2 is proportional to the quark mass m_q , see Eq.(7.4).

Moreover, the nonchiral neutral pion mass becomes negative for $eB > 0.6$ GeV, when the standard hyperfine cut-off of $\lambda \approx 1$ GeV $^{-1}$ is used, which might require a smaller λ . This fact calls for an additional investigation.

As for charged pions π , one can see in Fig.3 a drastically different behavior which has growing asymptotics of the type I according to (3.7) for chiral ($m_\pi^2 = O(m_q^2)$, lower curve) and nonchiral ($m_\pi^2 = O(\sigma)$ higher curve), cases. One can see in Fig.3 a reasonable agreement of lower curve with the lattice data of [14] while our present lattice data in Fig.3 correspond to much larger m_q and therefore are shifted upwards.

Turning to the ρ mass trajectories, one must remember our classification in Section 6, which implies, that both π^0, ρ^0 lines split into $(u\bar{u})$ and $(d\bar{d})$ species and the growing trajectories are proportional to $\sqrt{|e_q|B}$, yielding for those a ratio equal to $\sqrt{2}$.

The $\rho^0(s_z = 1, -1)$ PIH trajectories in Fig.5 and 6 agree well with our lattice data and with lattice data from [27], as well as $\pi^0(u\bar{u})$ and $\pi^0(d\bar{d})$ trajectories.

Note the difficulty in lattice evaluation of the $\rho^0(s_z = 0)$ lines which mix with the

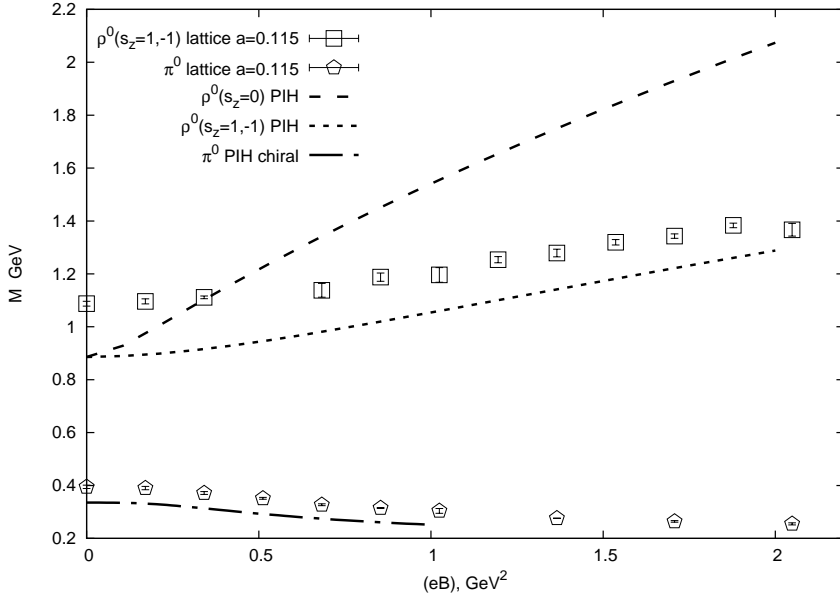


Figure 6. Mass evolution of $(\pi^0, \rho^0)(d\bar{d})$ quartet in MF from our analytic (PIH) and lattice data with $a = 0.115 \text{ fm}$.

much lower π^0 trajectories.

A very interesting situation occurs for $\rho^-(\rho^+)$ mass trajectories, presented in Fig.7. Only one of those belong to the ZHS type and tends to a constant at large MF, and both lattice and analytic curve agree within our accuracy $O(15\%)$, approximately the same kind of agreement is seen in Fig.7 for the trajectory of the type *I*, $\rho^-(s_z = 0)$ and that of the type *II*, $\rho^-(s_z = 1)$. Summarizing, one can conclude, that our lattice data agree with analytic predictions within our accuracy limits and our classification and theory based on the PIH formalism for all s -wave π, ρ mesons give a realistic physical picture in this section.

Acknowledgements

The authors are grateful to O.V. Teryaev for discussion. The analytic calculations were provided by M.A.Andreichikov, B.O.Kerbikov and Yu.A.Simonov with support by the Russian Science Foundation grant 16-12-10414. The lattice calculations (Section VIII) are presented in this paper were provided by E.V.Lushevskaya and O.E.Solovjeva with support by the RScF grant 16-12-10059.

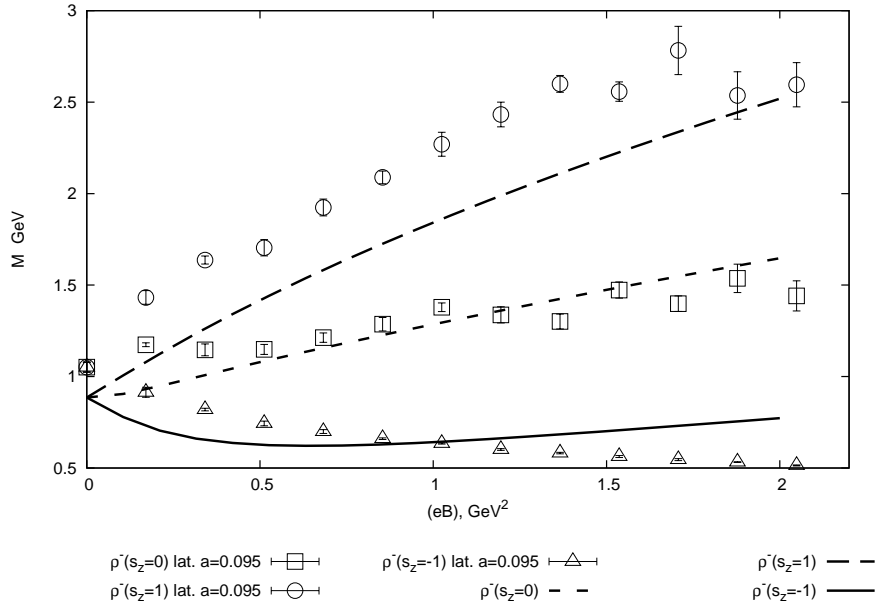


Figure 7. The ρ^- meson mass evolution in MF from our analytic (PIH) and lattice data with $a = 0.095 \text{ fm}$.

A String tension renormalization in CS method

The string tension renormalization procedure could be illustrated by an analogy from classical mechanics, where two point masses are connected by the spring with the following classical Lagrangian

$$L = \frac{m_1 \dot{x}_1^2}{2} + \frac{m_2 \dot{x}_2^2}{2} - \frac{k(x_1 - x_2)^2}{2}. \quad (\text{A.1})$$

In what follows we take substitution $m_1 = \omega_1$, $m_2 = \omega_2$ and $k = \frac{\sigma}{2\gamma}$, which makes the Lagrangian (A.1) canonically conjugated to the relativistic Hamiltonian (2.1) with the confinement potential was taken in oscillator form (2.6) at $B = 0$ up to momenta- and coordinate-independent terms. The Lagrangian could be canonically quantized in c.m. reference frame

$$E = \frac{P^2}{2M} + \frac{1}{2} \sqrt{\frac{k}{\mu}} (2n + 1); \quad E_0 = \frac{1}{2} \sqrt{\frac{k}{\mu}}, \quad P = 0, \quad (\text{A.2})$$

where E_0 is ground state. On the other hand, one can describe the same system as two independent oscillators with opposite phases (for $P = 0$), each of them is connected to the c.m. with its own spring, with Lagrangian

$$L = \frac{m_1 \dot{x}_1^2}{2} + \frac{m_2 \dot{x}_2^2}{2} - \frac{k_1 x_1^2}{2} - \frac{k_2 x_2^2}{2}, \quad (\text{A.3})$$

where the stiffnesses are $\frac{k_1}{k_2} = \frac{m_1}{m_2}$. To proceed further with canonical quantization procedure, one has for ground the state energy for (A.3)

$$E = \frac{P_z^2}{2M} + \frac{1}{2} \sqrt{\frac{k_1}{m_1}} (2n_1 + 1) + \frac{1}{2} \sqrt{\frac{k_2}{m_2}} (2n_2 + 1);$$

$$E_0 = \frac{1}{2} \sqrt{\frac{k_1}{m_1}} + \frac{1}{2} \sqrt{\frac{k_2}{m_2}}; \quad n_1 = n_2 = 0.$$
(A.4)

The expression (A.4) should take into account that in the quantum case the phases of two harmonic oscillators should be entangled due to constraint $m_1 x_1 + m_2 x_2 = 0$. An explicit derivation of the "σ-renormalization" requires Dirac quantization formalism for constrained systems. Here we use an heuristic way, based on the correspondence principle. One can substitute the constraint $m_1 x_1 + m_2 x_2 = 0$ and $\frac{k_1}{k_2} = \frac{m_1}{m_2}$ to the Lagrangian (A.3) with the result

$$L = L_1 = \frac{M}{m_2} \left(\frac{m_1 \dot{x}_1^2}{2} - \frac{k_1 x_1^2}{2} \right) = L_2 = \frac{M}{m_1} \left(\frac{m_2 \dot{x}_2^2}{2} - \frac{k_2 x_2^2}{2} \right).$$
(A.5)

In addition one could combine L_1 and L_2 to $L = \alpha L_1 + (1 - \alpha) L_2$, $\alpha \in [0, 1]$ which has the same energy and preserves number of degrees of freedom. If one take $\alpha = \frac{1}{2}$, the conjugated to L Hamiltonian is

$$H = p_1 \dot{x}_1 + p_2 \dot{x}_2 - L =$$

$$\frac{2m_2}{M} \left(\frac{p_1^2}{2m_1} + \left(\frac{M}{2m_2} \right)^2 \frac{k_1 x_1^2}{2} \right) + \frac{2m_1}{M} \left(\frac{p_2^2}{2m_2} + \left(\frac{M}{2m_1} \right)^2 \frac{k_2 x_2^2}{2} \right)$$
(A.6)

and after the canonical quantization procedure one has a ground state energy for (A.6)

$$E = \frac{2m_2}{M} \frac{1}{2} \sqrt{\left(\frac{M}{2m_2} \right)^2 \frac{k_1}{m_1}} + \frac{2m_1}{M} \frac{1}{2} \sqrt{\left(\frac{M}{2m_1} \right)^2 \frac{k_2}{m_2}}$$
(A.7)

The ground state energy (A.7) equals to (A.2) if one redefines k_1 and k_2 as

$$k_1 = \frac{k}{1 + \frac{m_1}{m_2}}; \quad k_2 = \frac{k}{1 + \frac{m_2}{m_1}}.$$
(A.8)

The resulting ground state energies, obtained with CS method and "σ-renormalization" procedure exactly coincide with the corresponding energies for the neutral mesons in the Pseudomomentum technique [41] in a whole range of MF, see e.g. (2.12-2.14) in the main text of the paper.

B The wave function of the neutral meson in CS method

One can suppose that the results for the averaged operator (4.3) for neutral mesons coincides with the exact one from [41] with Pseudomomentum technique in strong MF

regime ($eB \gg \sigma$) because of one-to-one correspondence for dynamical masses in Section 2. However, there is a difference about 30% (especially for ZHS states) because of the c.m. fixing procedure, i.e. the translational invariance breaking in CS method (see Section 2). The nature of this discrepancy is the lowest Landau level (LLL) degeneracy in angular momentum projection m in symmetric gauge, when MF is strong enough to make the confinig force negligible. Let's consider the Hamiltonian for a single particle in MF to illustrate this statement

$$H = \frac{1}{2m} \left(\hat{\mathbf{p}} - \frac{e}{2} \mathbf{B} \times \mathbf{x} \right)^2. \quad (\text{B.1})$$

The corresponding spectrum for this Hamiltonian is

$$E = \Omega(2n + |m| - m + 1), \quad (\text{B.2})$$

where $\Omega = \frac{eB}{2m}$ is cyclotron frequency, n is oscillator quantum number and m is an angular momentum projection to the direction of the MF. It's clear that there is an infinite degeneracy for LLL $n = 0$ for $m = 0, 1, 2, \dots$. If we go to the complex coordinates $z = x + iy$, the wave function for the ground state could be written as

$$\psi_0^{(m)} = \sum_m A_m (z^*)^m e^{-\frac{z^*z}{4}(eB)}, \quad (\text{B.3})$$

where A_m is an arbitrary constant. Extending this formalism to the case of two non-interacting particles with opposite charges in MF, one can write two-particle ground state wave function

$$\psi_0 = \sum_{m_1, m_2} A_{m_1, m_2} (z_1^*)^{m_1} (z_2)^{(m_2)} e^{-\frac{z_1^*z_1}{4}(eB) - \frac{z_2^*z_2}{4}(eB)}, \quad (\text{B.4})$$

Here we also rewrite the exact wave function for the neutral meson from [41] was got with Pseudomomentum procedure

$$\psi_0^{(p)} = \frac{1}{\sqrt{\pi^{3/2} r_\perp^2 r_z}} e^{-\frac{\eta_\perp^2}{2r_\perp^2} - \frac{\eta_z^2}{2r_z^2}}, \quad (\text{B.5})$$

where radii and their asymptotics in $eB \rightarrow \infty$ regime are

$$\begin{aligned} r_\perp &= \sqrt{\frac{2}{eB}} \left(1 + \frac{4\sigma\tilde{\omega}^{(0)}}{\gamma^{(0)}(eB)^2} \right)^{-\frac{1}{4}} \rightarrow \sqrt{\frac{2}{eB}}, \\ r_z &= \left(\frac{\gamma^{(0)}}{\sigma\tilde{\omega}^{(0)}} \right)^{\frac{1}{4}} \rightarrow \frac{1}{\sqrt{\sigma}} \end{aligned} \quad (\text{B.6})$$

Comparing transversal parts of the wave functions for CS method (2.18) as (f) and Pseudomomentum method as (p) in strong MF for ZHS meson

$$\begin{aligned}\psi_f^\perp(eB \gg \sigma) &\sim e^{-\frac{eB}{4}[(\mathbf{x}_1^\perp)^2 + (\mathbf{x}_2^\perp)^2]}, \quad v_s \\ \psi_p^\perp(eB \gg \sigma) &\sim e^{-\frac{eB}{4}(\mathbf{x}_1^\perp - \mathbf{x}_2^\perp)^2} = \psi_f(eB \gg \sigma)e^{-\frac{eB}{4}(\mathbf{x}_1 \cdot \mathbf{x}_2)}.\end{aligned}\tag{B.7}$$

It's evident that the term $\exp\{-\frac{eB}{4}(\mathbf{x}_1 \cdot \mathbf{x}_2)\}$ in (B.7) is formed by the power series in m_1 and m_2 entering before the exponent in (B.4). So, the difference between the CS wave function ψ_f and the exact wave function ψ_p is given by the superposition of the degenerate LLL basis wave functions. This additional term in (B.7) gives about 30% of the total value of the CS Coulomb integral (4.3) for neutral mesons. The nature of this underestimation is clear - an additional term in (B.4) recovers translational invariance of the c.m. for the ψ_f wave function. Also one should note that this correction doesn't exist for the charged meson case because of lack of the c.m. translational invariance due to c.m. precession in MF. The final step is to add an additional multiplier $\exp\{-\frac{eB}{4}(\mathbf{x}_1 \cdot \mathbf{x}_2)\}$ to our CS wave function (2.18) by hand according to previous speculations. This modification gives us 10% accuracy for the Coulomb correction integral (4.3) in comparison with one was obtained in [41].

References

- [1] D.E.Kharzeev, K.Landsteiner, A.Schmitt, H.-U.Yee, "Strongly interacting matter in magnetic fields", Lect. Notes Phys. **871**, (2013), (Springer); arXiv:1211.6245; V.A.Miransky and I.A.Shovkovy, Phys. Rept. 576, 1 (2015).
- [2] J.M.Lattimer and M.Prakash, Phys. Rept. **442**, 109 (2007); A.Y.Potekhin, Phys. Uspekhi **53**, 1235 (2010); Dong Lai, Space. Sci. Rev. **191**, 13 (2015); A.K.Harding and D. Lai, Rept. Prog. Phys. **69**, 2631 (2006).
- [3] D. Grasso and H. Rubinstein, Phys. Rept. **348**, 163 (2001).
- [4] S.Godunov, B.Machet, M.Vysotsky, Phys. Rev. **D85**, 044058 (2013), arXiv:1112.1891; M.I.Vysotsky, S.I.Godunov, Phys. Uspekhi **57**, p.194-198 (2014).
- [5] A.Shabad, V.Usov, Phys. Rev. Lett. **98**, 180403 (2007), Phys. Rev. **D73**, 125021 (2006).
- [6] B.M.Karnakov, V.S.Popov, JETP **97**, 890 (2003), JETP **141**, 5 (2012), Phys. Uspekhi **57** p.257-279 (2014).
- [7] M.A.Andreichikov, B.O.Kerbikov, Yu.A.Simonov, JETP Lett **99**, 5, p.289 (2014).
- [8] D.E.Kharzeev, L.D.McLerran and H.J.Warringa, Nucl. Phys. **A803**, 227 (2008); V.Skokov, A.Illarionov and V.Toneev, Int. J. Mod. Phys. **A24**, 5925 (2009).
- [9] T.Tajima, Eur. Phys. J. D **55**, 519 (2009).
- [10] K.Hattori, T.Kojo, Nan Su, Nucl. Phys. **A951**, p.1-30 (2016).

- [11] F.X.Lee, L.Zhou, W.Wilcox and J.Christenson, arXiv: hep-lat/0509065; P.Haegler, Phys. Rep. **490**, 49 (2010); arXiv:0912.5483.
- [12] T.Primer, W.Kamleh, D.Leinweber and M.Burkardt, arXiv: 12112.1963 [hep-lat].
- [13] E.V.Lushevskaya and O.V.Larina, arXiv:1203.5699 [hep-lat]; JETP Lett. **98**, 11, p.652 (2014), arXiv:1306.2936.
- [14] G.S.Bali, F.Bruckmann, G.Enrödi, et al., JHEP **1202**, 044 (2012).
- [15] M.D'Elia, S.Mukherjee and F.Sanfilippo, Phys. Rev. D **82**, 051501 (2010); arXiv:1005.5365; M.D'Elia and F.Negro, Phys. Rev. D **83**, 114028 (2011); arXiv:1103.2080; M.D'Elia, arXiv:1209.0374.
- [16] P.Buividovich, M.Chernodub, E.Lushevskaya and M.Polikarpov, Phys. Lett. B **682**, 484 (1010); arXiv:0812.1740; V.Braguta, P.Buividovich, T.Kalaydzhyan, S.Kusnetsov and M.Polikarpov, PoS Lattice 2010, 190 (2010); arXiv:1011.3795.
- [17] E.-M.Ilgenfritz, M.Kalinowski, M.Muller-Preussker, B. Peterson and A.Schreiber, Phys. Rev. D **85**, 114504 (2012); arXiv:1203.3360.
- [18] Yu.A.Simonov, Phys. Atom. Nucl. **67**, 1027 (2004), arXiv:hep-ph/0305281.
- [19] E.V. Lushevskaya, O.E. Solovjeva, O.E. Kochetkov and O.V. Teryaev, Nuclear Physics B **898**, 627 (2015).
- [20] E.V. Lushevskaya, O.E. Kochetkov, O.V. Teryaev and O.E. Solovjeva, JETP Letters **101**, Issue 10, 674 (2015).
- [21] E.V.Lushevskaya, O.E.Solovjeva, O.V.Teryaev, arXiv:1608.03472 (2016).
- [22] E.V.Lushevskaya, O.E.Solovjeva, O.V.Teryaev, Phys. Lett. **B761**, p.393 (2016).
- [23] E.V.Lushevskaya, O.A.Kochetkov, O.V.Larina, O.V.Teryaev, Nucl. Phys. **B884**, p.1-16 (2014).
- [24] O.V.Teryaev, Int. J. Mod. Phys. Conf. Ser. **39**, 1560083 (2015).
- [25] C.Bonati, M.D'Elia, A.Rucci, Phys. Rev. **D92**, 054014 (2015).
- [26] H. Neuberger, Phys. Lett. B **417**, 141 (1998), arXiv: hep-lat/9707022.
- [27] Y.Hidaka, A.Yamamoto, Phys. Rev. **D87**, 094502 (2013), arXiv:1209.0007.
- [28] G.Bali, B.B.Brandt, G.Endrodi, B.Glassle, 33rd International Symposium on Lattice field theory, 14-18 Jul 2015, Kobe, Japan, arXiv:1510.03899.
- [29] F.X.Lee, S.Moerschbacher, W.Wilcox, Phys. Rev. **D78**, 094502 (2008), arXiv:0807.4150.
- [30] I. A. Shushpanov and A. V. Smilga, Phys. Lett. **B402**, 351 (1997).
- [31] N. O. Agasian and I. A. Shushpanov, JETP Lett. **70**, 717 (1999); Phys. Lett. **B472**, 143 (2000); JHEP **0110**, 006 (2001).
- [32] N. O. Agasian, Phys. Lett. **B488**, 39 (2000); Phys. Atom. Nucl. **64**, 554 (2001).

- [33] J. O. Andersen, JHEP, **1210**, 005 (2012); Phys. Rev. **D86**, 025020 (2012).
- [34] T. M. Aliev, A. Ozpineci, and M. Savci, Phys. Lett. B **678**, 470 (2009); arXiv: 0902.4627 [hep-ph];
T. M. Aliev, K. Azizi, and M. Savci, J. Phys. G **37**, 075008 (2010);
H. M. Choi and C. R. Ji, Phys. Rev. D **70**, 053015 (2004);
J. P. B. de Melo and T. Frederico, Phys.Rev. C **55**, 2043 (1997).
M.S.Bhagwat and P.Maris, Phys. Rev. **C77**, 025203 (2008).
- [35] J.N.Heddith, W.Kamlech, B.Lasscock, D.B.Leinweb, G.W.Williams, J.M.Zanotti, Phys. Rev. **D75**, 094504 (2007), arXiv:hep-lat/0703014.
- [36] J.Alford, M.Strickland, Phys. Rev. **D88**, 105017 (2013), arXiv:1309.3003.
- [37] C.S.Machado et. al., Phys. Rev. **D88**, 034009 (2013), arXiv:1305.3308.
- [38] M.Kawaguchi, S.Matsuzaki, arXiv:1511.06990 (2015).
- [39] S.Avancini, R.Farias, M.Pinto, W.Tawares, V.Timoteo, arXiv:1606.05754 (2016).
- [40] M. A. Andreichikov, B. O. Kerbikov, and Yu. A. Simonov, arXiv:1210.0227[hep-ph].
- [41] M. A. Andreichikov, B. O. Kerbikov, V. D. Orlovsky and Yu. A. Simonov, Phys. Rev. D. **87**, 094029 (2013); arXiv:1304.2533.
- [42] M. A. Andreichikov, V. D. Orlovsky and Yu.A.Simonov, Phys. Rev. Lett. **110** 162002 (2013); arXiv:1211.6568;
- [43] C.Bonati, M.D'Elia, M.Mariti and F.Negro, Phys. Rev. **D89**, 114502 (2014).
- [44] Yu.A.Simonov, M.A.Trusov, Phys. Lett. **B747** 48-52 (2015), arXiv:1503.08531
- [45] Yu.A.Simonov, Phys. Rev. D **88**, 025028 (2013); arXiv:13.03.4952.
- [46] Yu.A.Simonov, Phys. Rev. D. **88**, 053004 (2013); arXiv:1304.0365.
- [47] V.D.Orlovsky and Yu.A.Simonov, JHEP, **1309**, 135(2013); arXiv:1306.2232.
- [48] Yu.A.Simonov, Phys. Rev. **D65**, 094018 (2002).
- [49] Yu.A.Simonov, Int. J. Mod. Phys. /bf 31, 1650016 (2016).
- [50] Yu.A.Simonov, Phys.At.Nucl. **79**, 277 (2016).
- [51] Yu.A.Simonov, Phys. Atom. Nucl. **74**, 1223 (2011), arXiv:1011.5386.
- [52] A.M.Badalian and Yu.A.Simonov, Phys. Rev. D **87**, 074012 (2013).
- [53] B. O. Kerbikov and Yu. A. Simonov, Phys. Rev. D **62**, 093016 (2000).
- [54] M.A.Andreichikov, B.O.Kerbikov, V.D.Orlovsky and Yu.A.Simonov, Phys. Rev. **D 89**, 074033 (2014); arXiv:1312.2212.
- [55] W. E. Lamb, Phys. Rev. **85**, 259 (1952); L.P.Gor'kov and I.E. Dzyaloshinskii, Soviet Physics JETP, **26**, 449 (1968);
J.E.Avron, I.W.Herbst, and B.Simon, Ann.Phys. (NY), **114**, 431 (1978);
H.Grotsch and R.A.Hegstrom, Phys. Rev. **A4**, 59 (1971).
- [56] Yu.A.Simonov,Phys. Lett B **719**, 464 (2013).

- [57] Yu.A.Simonov, Phys. Rev. **D88**, 053004 (2013).
- [58] B.O.Kerbikov, M.I.Polikarpov, L.V.Shevchenko, Nucl. Phys. **B331**, 19 (1990).
- [59] A.M. Badalian, B.L.G. Bakker, Phys. Rev. **D66**, 034025 (2002); Phys. Rev. **D84**, 034006 (2011);
A.M. Badalian, B.L.G.Bakker, Yu.A.Simonov, Phys. Rev. **D66**, 034026 (2002),
A.M.Badalian, B.L.G.Bakker, I.V.Danilkin, Phys. Rev. **D81**, 071502 (2010).
- [60] Yu.A.Simonov, Phys. Atom. Nucl. **79**, 455 (2016).
- [61] Yu.A.Simonov, Phys. Atom. Nucl. **76**, 525 (2013), arXiv:1205.0692.
- [62] Yu.A.Simonov, Phys. Atom. Nucl. **67**, 846 (2004), arXiv:hep-ph/0302090.
- [63] Yu.A.Simonov, Phys. Rev. **D65**, 094018 (2002).
- [64] Yu.A.Simonov, Int. J. Mod. Phys. **31**, 1650016 (2016).
- [65] Yu.A.Simonov, Phys. Atom. Nucl. **79**, 277 (2016).